One- and Two-Dimensional ESEEM Spectroscopy of Flavoproteins†

Jesús I. Martínez,‡ Pablo J. Alonso,‡ Carlos Gómez-Moreno,§ and Milagros Medina*,§

Instituto de Ciencia de Materiales de Aragón, Consejo Superior de Investigaciones Científicas−Universidad de Zaragoza, and Departamento de Bioquímica y Biología Molecular y Celular, Facultad de Ciencias, Universidad de Zaragoza, 50009 Zaragoza, Spain

Received June 23, 1997; Revised Manuscript Received September 15, 1997⊗

ABSTRACT: One- and two-dimensional (1D and 2D) electron spin echo envelope modulation (ESEEM) spectroscopy was applied to study the flavin cofactors in the neutral semiquinone states of flavodoxin and ferredoxin-NADP$^+$ reductase (FNR) from the cyanobacterium *Anabaena* PCC 7119, and the anionic semiquinone state of cholesterol oxidase from *Brevibacterium sterolicum*. High-resolution crystal structures are available for all these proteins. Three- and 4-pulse ESEEM and hyperfine sublevel correlation spectroscopy (HYSCORE) techniques at X-band were used. HYSCORE spectra showed correlations between transitions caused by interaction of the isoalloxazine unpaired electronic spin present in the semiquinone state with several nitrogen and hydrogen nuclei. Measurements of isotopic labeled samples ([^{15}N]FMN flavodoxin and [^{2}H]flavodoxin) allowed the assignment of all the detected transitions to nuclei belonging to the FMN cofactor group. Interactions of nitrogens in positions 1 and 3 of the isoalloxazine ring were determined to have isotropic hyperfine coupling constants in the 1−2 and 0.5−1 MHz ranges for all the different flavoprotein semiquinones studied. Information about the quadrupolar term of these nuclei was also obtained. An intense correlation in the negative quadrant was detected. It has been associated to the strongly interacting N(10) nucleus. The complete hyperfine term parameters (including the sign) were obtained from detailed analysis of this signal, being the quadrupolar parameter, *K*, also estimated. Another correlation in the HYSCORE spectra, corresponding to hydrogen bound to the N(5) position in neutral flavin semiquinones, was detected. Its interaction parameters were also determined. This study demonstrates that ESEEM spectroscopy, and in particular the HYSCORE technique, are of particular utility for detecting and assigning nuclear transition frequencies in flavoprotein semiquinones. Moreover, the results reported here are complementary to ENDOR studies, and both techniques together provide an important tool for obtaining information about spin distribution in the flavin ring of flavoproteins in the semiquinone state.

A large number of flavin-containing proteins have been uncovered to date, many of them being enzymes. Flavoproteins participate in a large number of oxidation/reduction reactions that function either in energy transduction or in biosynthesis and degradation of metabolic intermediates (Edmondson & McCormick, 1987; Yagi, 1993). This means that the same cofactor (the flavin) is able to take part in catalytic processes which must vary widely from the mechanistic point of view. The activation of a particular activity of the flavin results from its interaction with the protein polypeptidic chain at the active center, and, for most of the enzymes, a transfer of electrons must take place between the substrate and the flavin during the catalytic event. Due to their unique ability to transfer either one or two electrons, flavoproteins are used for electron transfer between pyridine (two-electron donor/acceptor) nucleotides and metal-containing heme or iron−sulfur clusters (one-electron donor/acceptor) present in proteins. They also participate in the transfer of electrons to other flavin-containing proteins, which raises interesting questions related to the thermodynamic and structural requirements for efficient flavin−flavin electron transfer. The involvement of flavin semiquinone intermediates in flavoenzyme-catalyzed reaction has been the focus of a large number of studies. In some enzymes it has already been shown that the semiquinone state is an important intermediate in the overall catalytic pathway (Janot et al., 1990; White et al., 1993). Nevertheless, a number of uncertainties about their participation in electron-transfer reactions in biological systems still remain (Edmondson & Tollin, 1983; Müller, 1983). In the present study we have deepened our knowledge of the semiquinone state of three flavoproteins, flavodoxin and ferredoxin-NADP$^+$ reductase (FNR) from *Anabaena* PCC 7119, both of them exhibiting a neutral semiquinone radical, and cholesterol oxidase from *Brevibacterium sterolicum*, which presents an anionic semiquinone.

The photochemical reduction of NADP$^+$ to NADPH has been shown to proceed via ferredoxin and the flavoenzyme FNR (Rogers, 1987; Knaff & Hirasawa, 1991). When cultures of cyanobacteria are deprived of iron, they synthesize a low-M_r FMN-containing protein, flavodoxin, which replaces ferredoxin in most reactions (Fillat et al., 1988). *Anabaena* PCC 7119 FNR has been extensively characterized (Pueyo & Gómez-Moreno, 1991; Pueyo et al., 1991). It has a molecular mass of 36 kDa and contains one mole of noncovalently bound FAD cofactor/mole of enzyme. The three-dimensional structure of *Anabaena* PCC 7119 FNR and that of a complex with NADP$^+$ have been recently solved at 1.8

† This work was supported by Grant BIO-94-0621-C02-01 from the Comisión Interministerial de Ciencia y Tecnología to C.G.-M.

* To whom correspondence should be addressed. Phone: +34-976-761279. Fax: +34-976-762123. E-mail: mmedina@posta.unizar.es.

‡ Instituto de Ciencia de Materiales de Aragón.

§ Departamento de Bioquímica y Biología Molecular y Celular.

⊗ Abstract published in *Advance ACS Abstracts,* November 1, 1997.

S0006-2960(97)01495-5 CCC: $14.00

and 2.25 Å, respectively (Serre et al., 1996). Redox titrations showed that the maximum proportion of *Anabaena* FNR semiquinone at equilibrium, in the pH range 6−8, was 29−12% (Pueyo et al., 1991). Nevertheless, in FNR, the FAD semiquinone state certainly plays a role in the enzyme-catalyzed reduction of $NADP^+$. Although the mechanism of this reaction has not been revealed, it is generally accepted that ferredoxin is a one-electron carrier and there is only a single ferredoxin-binding site on FNR. In this case, it is difficult to imagine mechanisms for electron transfer from reduced ferredoxin to the FAD of FNR that do not involve at least the transient formation of the FAD semiquinone state (Knaff & Hirasawa, 1991). Moreover, the structure of this protein is the prototype of a large family of flavin-dependent oxidoreductases that function as transducers between nicotinamide dinucleotides (two-electron carriers) and one-electron carriers (Karplus et al., 1991; Correll et al., 1993; Bruns & Karplus, 1995). Flavodoxin is isolated from *Anabaena* PCC 7119 vegetative cells when iron is limited in the culture medium (Fillat et al., 1988). It has a molecular mass of 20 kDa, contains 1 mol of FMN/mol of protein, and forms a 1:1 complex with FNR (Fillat et al., 1988, 1990). The semiquinone of FMN in flavodoxin is highly stable, so that close to 100% of the flavin is in this form after addition of one electron. This is a consequence of the relative midpoint potential for the oxidized/semiquinone couple (−212 mV) and the semiquinone/hydroquinone couple (−436 mV) (Pueyo et al., 1991).

Cholesterol oxidase is a flavin-dependent enzyme that catalyzes the oxidation and isomerization of 3β-hydroxysteroids having a double bond at $\Delta^5-\Delta^6$ of the steroid ring backbone (Smith & Brooks, 1975; Kamei et al., 1978; Inouye et al., 1982). The enzyme from the soil bacterium *B. sterolicum* is a monomeric oxidase containing one molecule FAD/molecule protein (Uwajima et al., 1974). The crystal structure of the enzyme from *B. sterolicum* has been determined at 1.8 Å resolution, both in the presence and in the absence of a bound steroid (Vrielink et al., 1991; Li et al., 1993). A significant structural homology has been observed between cholesterol oxidase and the members of the glucose−methanol−choline (GMC) oxidoreductases family (Caverner, 1992). This family of enzymes all undergo similar oxidative chemistry, namely, the flavin-assisted oxidation of an alcohol to an aldehyde or ketone function.

EPR spectroscopy has played an important role in the detection of flavin semiquinones, being particularly useful for distinguishing the anionic and neutral radicals. However, this technique provides little insight into the structure of protein-bound semiquinones because of the large number of unresolved anisotropic hyperfine couplings. Electron nuclear double resonance (ENDOR) spectroscopy offered improved spectral resolution and has provided information on the molecular structure and electronic distribution on model flavin and flavoprotein radicals (Kurreck et al., 1984, 1987; Edmondson, 1985; Bretz et al., 1987). Structural data on paramagnetic centers in biological systems have also been obtained by analyzing electron spin-echo envelope modulations (ESEEM) arising from the interaction with various nuclei (Tsvetkov & Dikanov, 1987). This technique is particularly sensitive to weak hyperfine interactions (Mims & Peisach, 1981). ENDOR and ESEEM spectroscopic characterizations of the semiquinone forms from flavodoxin and FNR from *Anabaena* PCC 7119, as well as from cholesterol oxidase from *B. sterolicum* have already been reported (Medina et al., 1994, 1995, 1997; Medina & Cammack, 1996). ENDOR studies of these flavoprotein semiquinones allowed to detect strong hyperfine couplings due to the 8-CH_3 and 6-CH protons in anionic (cholesterol oxidase) and neutral (flavodoxin and FNR) semiquinone forms. ENDOR spectroscopy has also shown that upon $NADP^+$ binding to FNR, a change in the electron density distribution on the flavin ring takes place, consistent with electron withdrawal by interaction with the nicotinamide ring (Medina et al., 1995). The same effect was observed when cholesterol oxidase was studied in the presence of its steroid substrate (Medina et al., 1994). Recent three-pulse 1D-ESEEM studies on the frozen solution of cholesterol oxidase, flavodoxin, and FNR semiquinones at X-band showed prominent nuclear modulation frequencies. These frequencies seem to be consistent with the presence of at least one ^{14}N magnetically coupled to the paramagnet and could be interpreted as arising from nitrogens at positions 1 and/or 3 of the flavin ring system (Medina & Cammack, 1996; Medina et al., 1997; Edmondson et al., 1990).

Difficulties in associating 1D-ESEEM features to each nucleus, as well as those arising from working with orientationally disordered samples, can be overcome by using 2D techniques. Four pulse 2D-HYSCORE spectroscopy provides correlations between nuclear transition frequencies belonging to different manifolds of a single electronic spin (Höfer et al., 1986). It has been proved to be very useful for assignment of ESEEM signals and for the examination of broad signals which are too weak to be detected in 1D-ESEEM experiments, as occurs for orientationally disordered samples in the case of anisotropic interactions (Shane et al., 1994; Kofman et al., 1995). Recently, the HYSCORE technique has already been successfully applied to the study of the metal ligand environment in different proteins (Shergill et al., 1995; Kofman et al., 1996; Dikanov et al., 1996).

In the present study we have characterized the neutral semiquinone states of flavodoxin and FNR from *Anabaena* PCC 7119, and the anionic semiquinone state of cholesterol oxidase from *B. sterolicum*, using three-pulse (3P) and four-pulse (4P) 1D-ESEEM and 2D-HYSCORE techniques. To our knowledge this is the first report on a flavoprotein semiquinone HYSCORE study. We show that 1D-ESEEM signals assigned to weakly interacting nitrogen in cholesterol oxidase, flavodoxin, and FNR semiquinones (Medina et al., 1997; Medina & Cammack, 1996) are readily detected by HYSCORE spectroscopy. Detailed information about hyperfine and quadrupolar interaction terms is also reported. From our 1D-ESEEM and HYSCORE experiments we can get new, valuable data about spin density in the pyrimidine and pyrazine rings of the flavin. The characterization of flavoprotein semiquinones by these techniques opens more

[1] Abbreviations: EPR, electron paramagnetic resonance; ENDOR, electron nuclear double resonance; ESEEM, electron spin-echo envelope modulation; FFT, fast Fourier transform; HYSCORE, hyperfine sublevel correlation spectroscopy; [^{15}N]FMN flavodoxin, flavodoxin sample in which the FMN cofactor has been replaced by a FMN molecule in which all nitrogens are ^{15}N; [^{2}H]flavodoxin; flavodoxin sample in which exchangeable ^{1}H have been replaced by ^{2}H; a, isotropic hyperfine coupling constant; T, anisotropic hyperfine coupling constant; T_M, short phase memory time; dq, double quantum; sq, single quantum; ν_L, nuclear Zeeman frequency; e^2qQ, quadrupole coupling constant; q, quadrupolar interaction; K, quadrupolar parameter; η, asymmetry parameter; hf, hyperfine.

possibilities in the study of the environment of the flavin cofactor in proteins and in the modulation of its properties by the apoprotein.

MATERIALS AND METHODS

Biological Material

Anabaena PCC 7119 flavodoxin had been previously cloned in the pTrc99a plasmid and expressed in *Escherichia coli* PC 2495 strain. Cell culture, protein induction, isolation and reconstitution with FMN was as previously described (Fillat et al., 1991; Genzor et al., 1996). FNR was purified from *E. coli* PC 0225 strain transformed with the FNR gene as previously described (Gómez-Moreno et al., 1995). Cholesterol oxidase from *B. sterolicum* was isolated and purified using the methods described by Uwajima et al. (1973). To prepare ^{15}N-labeled FMN a culture of *E. coli* containing the *Anabaena* flavodoxin gene was grown in SV minimal medium using $^{15}NH_4Cl$ (enrichment in ^{15}N >99.5%) as the only nitrogen source. ^{15}N-labeled flavodoxin was purified as described for unlabeled protein (Fillat et al., 1991), and its ^{15}N-labeled FMN was extracted by precipitation of the apoprotein component with trichloroacetic acid (Genzor et al., 1996). The supernatant, containing the ^{15}N-labeled FMN, was neutralized and used as described below. Since unlabeled antibiotic was also used during the cultures, the enrichment on ^{15}N of the ^{15}N-labeled FMN prepared for apoflavodoxin reconstitution was estimated uniform and over 92%. Unlabeled apoflavodoxin was prepared by removal of the FMN group by treatment of the holoprotein with trichloroacetic acid (Genzor et al., 1996). Apoflavodoxin was solved in buffer and dialyzed to remove the acid. Reconstitution with ^{15}N-labeled FMN was followed spectrophotometrically by titration of the apoflavodoxin with the obtained [^{15}N]FMN.

Samples were transferred into the desired buffer (usually 10 mM HEPES, pH 7, or HEPES-D_2O, pD 7) by dilution and ultrafiltration through Centricon 10 microconcentrators (Amicon, Witten-Herdecke), at 4 °C. The cycle was repeated three times, to give a final buffer enrichment of 95−99%.

HYSCORE Sample Preparation

Flavodoxin, FNR and cholesterol oxidase samples were reduced anaerobically to the semiquinone state at 4 °C by light irradiation with a 150 W Barr & Stroud light source, approximately 7.5 cm from the sample, in the presence of 20 mM EDTA and 2.5 μM 5-deazariboflavin. Maximal production of semiquinone was obtained by taking samples and recording EPR spectra during the illumination process. Samples (400−800 μM protein) were prepared in a sealed glass vessel under argon and transferred anaerobically using a gas-tight microsyringe into the EPR tubes, which were immediately frozen in liquid nitrogen. To avoid oxygen introduction during sample transfer, the EPR tubes were connected to the vessel through a lateral arm and flushed with argon prior to sample withdrawal. The samples containing the highest proportion of semiquinone state were used for ESEEM measurements. The samples were stored in liquid nitrogen, or at −70 °C, until use.

Spectroscopic Measurements

A Bruker ESP380E spectrometer operating in X-band (9−10 GHz) was used for pulsed-EPR measurements. Spectra were taken at a temperature of 15 K. The static magnetic field was set at about 347 mT, and the microwave frequency was 9.75 GHz. Field position was selected in the center of the EPR signal to give a maximum echo intensity. Orientation selection effects are not expected provided that EPR signals are narrow (peak-to-peak width less than 2 mT) and the main contribution to their width comes from unresolved hyperfine interactions. Microwave pulse sequences were ($\pi/2-\tau-\pi/2-t_1-\pi/2$) for 3P ESEEM, ($\pi/2-\tau-\pi/2-t_1-\pi-t_1-\pi/2$) for 4P ESEEM, and ($\pi/2-\tau-\pi/2-t_1-\pi-t_2-\pi/2$) for HYSCORE experiments. In each case, appropriate phase cycling was applied to remove unwanted echoes. For 3P experiments microwave pulses were set 16 ns long, whereas for 4P experiments both $\pi/2$ and π pulses were set 24 ns long. In 1D experiments, τ was fixed in a typical value of 144 ns and 1024 points were collected, varying t_1 with a step of 8 ns. τ was selected to be 96 ns in HYSCORE experiments, and spectra varying t_1 and t_2 independently had (256, 256) points. Typical steps for t_1 and t_2 were 16 ns. HYSCORE spectra with steps of 32 ns were also recorded to improve resolution in the low-frequency region. ESEEM signal of our samples at 15 K was quite intense but shot repetition time should be large (about 25 ms) in order to avoid saturation effects.

Data Handling/Analysis

Frequency domain spectra were obtained using the WIN-EPR program from Bruker in the following way: the base line was subtracted in the time domain spectrum, windowing with a square sine bell function was applied for enlarging the signal:noise ratio, and a fast Fourier transform (FFT) algorithm was then applied, being the modulus of the result the frequency spectrum. To analyze our results the 3P 1D-ESEEM signal of $I = 1$ nuclei was simulated using a computer program developed at the University of Nijmegen by E. J. Reijerse. Nuclear transition frequencies and HYSCORE signal intensities for $I = {}^1/_2$ nuclei signals were calculated using the expressions given by Dikanov and Tsvetkov (1992a).

EXPERIMENTAL RESULTS

Different ESEEM experiments have been applied to the study of the semiquinone states of flavodoxin, FNR, and cholesterol oxidase. Two-pulse ($\pi/2-\tau-\pi$) 1D-ESEEM spectra are poorly resolved due to the short phase memory time, T_M, of the systems. Nevertheless, well-resolved 3P and 4P 1D-ESEEM spectra can be obtained. 3P spectra show nuclear transition main frequencies, whereas 4P spectra also produce peaks corresponding to "combination frequencies" (Schweiger, 1990). Figure 1A shows the 3P 1D-ESEEM spectra recorded for the semiquinone states of cholesterol oxidase, FNR, flavodoxin, [^{15}N]FMN flavodoxin and [^{2}H]-flavodoxin. The corresponding 4P 1D-ESEEM spectra are shown in Figure 1B. A narrow intense peak in the 3 MHz region is detected for all the three samples with natural abundant isotopes in 3P and 4P 1D-ESEEM experiments. Other less intense features can also be seen in the low-frequency region, 0−5 MHz. In cholesterol oxidase semiquinone a peak at 2.2 MHz also appears. This peak is not seen in the spectra recorded for FNR and flavodoxin semiquinones. FNR shows a second peak in the 3.5 MHz region. 4P experiments show (combination) peaks in the 6−8 MHz region for these samples. When higher frequency

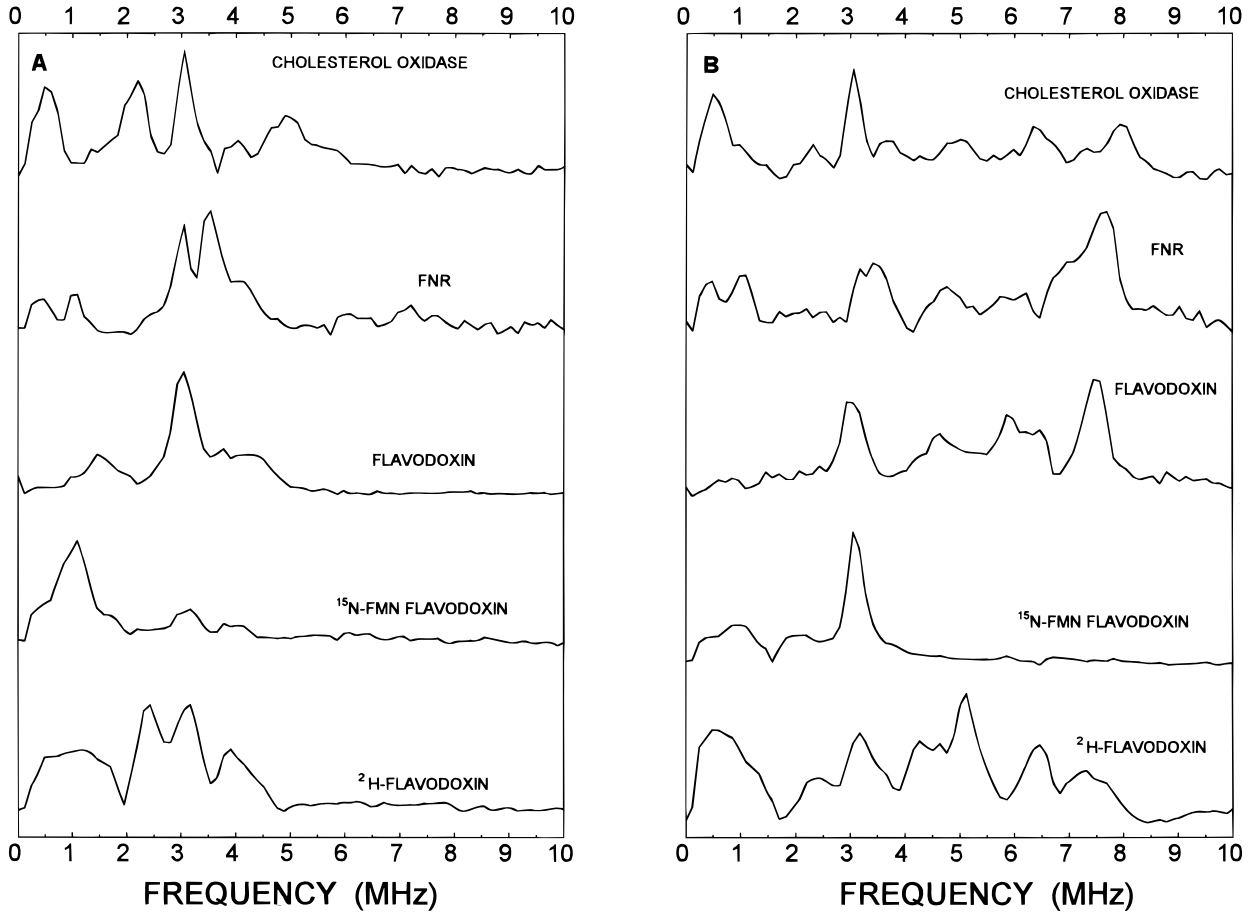

FIGURE 1: Fourier transform 3P (A) and 4P (B) 1D-ESEEM spectra of the different flavoprotein samples in the semiquinone state. τ value was 144 ns (for experimental conditions see Materials and Methods).

regions were studied, two more peaks, about 15 and 30 MHz, are detected (not shown) in all the samples. These frequency values correspond to the ^{1}H Larmor frequency and twice this frequency, respectively. Flavodoxin and FNR semiquinone 4P experiments also show a less intense peak in the 33 MHz region.

The low-frequency region of [^{15}N]FMN flavodoxin semiquinone 3P spectrum shows a dominating broad feature about 1 MHz. Moreover, in these spectra the features present in the unlabeled FMN flavodoxin semiquinone spectra are clearly diminished in comparison with the 1 MHz peak. It is also noticeable that no combination peaks at the 6−8 MHz region are detected in the 4P experiment for the [^{15}N]FMN flavodoxin semiquinone and that a peak at 3 MHz is the most prominent in this spectrum.

[^{2}H]Flavodoxin semiquinone 3P experiment spectra show a broad structure between 0.5 and 1.5 MHz and a peak at 2.4 MHz. The spectra above the 3 MHz region resemble to those of unlabeled flavodoxin semiquinone. In the 4P spectrum an intense (combination) peak at 5 MHz is seen.

Two-dimensional HYSCORE spectra for the five different semiquinone samples studied are presented in Figures 2−4. Features shown in the diagonals are due to unwanted echoes or to weakly interacting nuclei. Out-of-diagonal signals correspond to correlations between frequencies of transitions belonging to different manifolds of the same unpaired electronic spin. The main correlation features (peaks and ridges) detected in the spectra are summarized here:

(a) A curved ridge in the positive quadrant, roughly perpendicular to the diagonal, centered about (7 MHz, 26 MHz). This feature is clearly displayed in the flavodoxin and the [^{15}N]FMN flavodoxin semiquinone HYSCORE spectra, can be distinguish over the noise level in the FNR semiquinone spectrum, and does not appear at all in the cholesterol oxidase and the [^{2}H]flavodoxin semiquinone spectra.

(b) Two narrow, intense, hardly resolved, peaks in the region (3 MHz, 5 MHz) (positive quadrant). This feature can be seen in the spectra of all semiquinone samples, but the [^{15}N]FMN flavodoxin semiquinone spectrum shows these peaks clearly diminished with regard to those shown for unlabeled flavodoxin semiquinone. Besides, for the [^{15}N]-FMN flavodoxin semiquinone sample another pair of correlation peaks about (1 MHz, 2 MHz) appears.

(c) A curved correlation ridge in the negative quadrant, approximately parallel to the diagonal. The shape of this feature only shows small differences in the spectra obtained for flavodoxin, FNR, and cholesterol oxidase semiquinones. No changes were detected for this ridge when studying the HYSCORE spectrum of [^{2}H]flavodoxin semiquinone. Nevertheless, the negative quadrant ridge in the HYSCORE spectrum of [^{15}N]FMN flavodoxin semiquinone shows a very different shape and length when compared with the ridges found in the rest of flavoprotein semiquinone spectra.

DISCUSSION

The aromatic nature of the heterocyclic flavin ring system allows a distribution of spin density to be expected. A

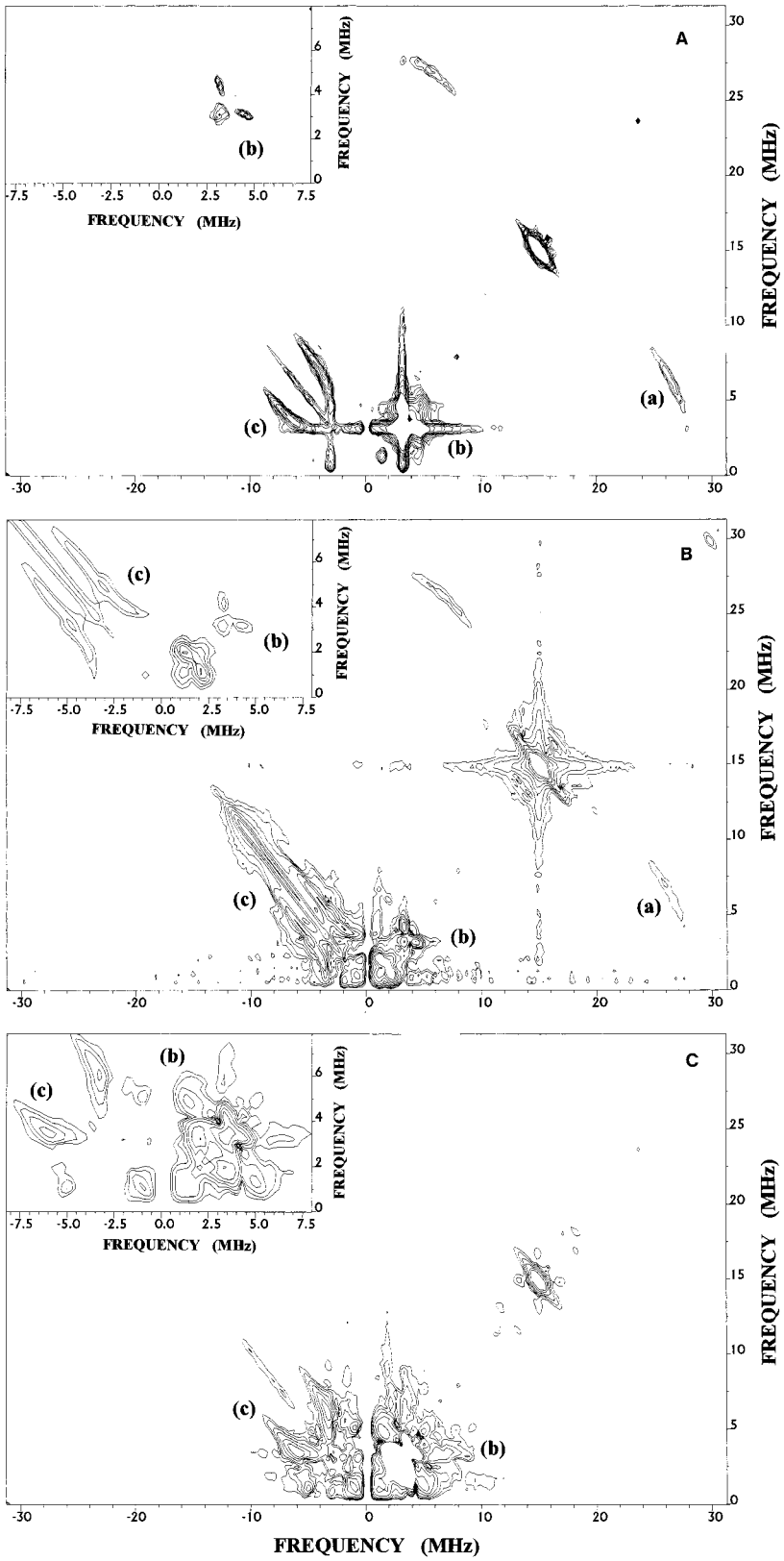

FIGURE 2: 2D-HYSCORE spectra of different flavodoxin samples in the semiquinone state. (A) Flavodoxin semiquinone, (B) [^{15}N]FMN flavodoxin, and (C) [^{2}H]flavodoxin (for experimental conditions see Materials and Methods). The main features are marked from (a) to (c) (see text). Insets display enlargements of the HYSCORE spectra in the (0;6.5 MHz, 0;6.5 MHz) region for (A), and the (−6.5;6.5 MHz, 0;6.5 MHz) region for B and C.

knowledge of sites of high spin density is of mechanistic importance, since it can suggest potential positions where electron transfer could occur in flavoenzyme catalyzed reactions involving the semiquinone intermediate. The flavin radicals can occur in different protonation states, i.e., cationic, neutral, and anion radical. In model compounds the protonation state present in the semiquinone state depends on the pH of the solution. In flavoproteins, only the presence of neutral and anionic flavin semiquinones has been detected, the species formed being determined by the interaction of

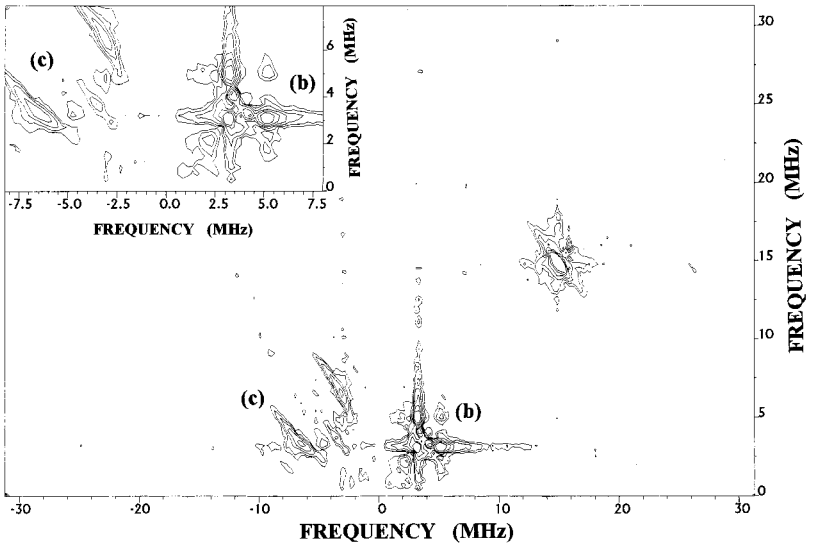

FIGURE 3: 2D-HYSCORE spectrum of cholesterol oxidase in the semiquinone state (for experimental conditions see Materials and Methods). The main features are marked from (a) to (c). The inset shows the (0−6.5 MHz, 0−6.5 MHz) region enlarged.

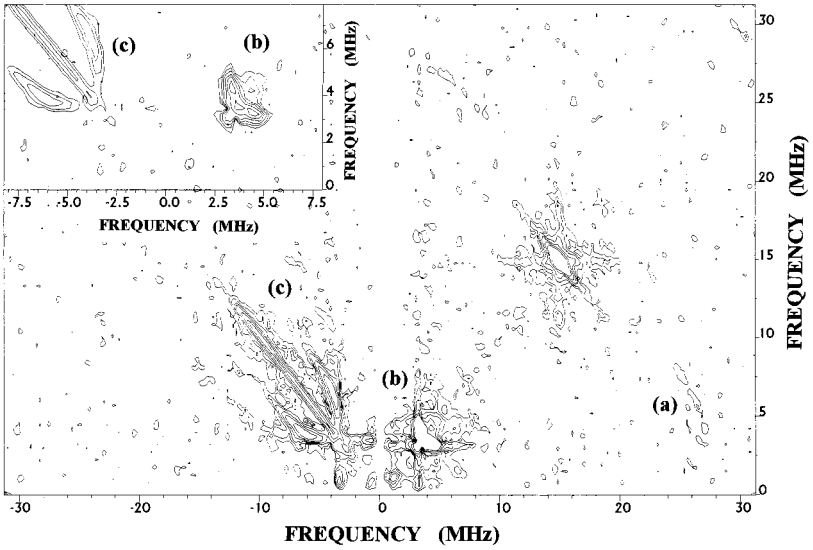

FIGURE 4: 2D-HYSCORE spectrum of FNR in the semiquinone state (for experimental conditions see Materials and Methods). The main features are marked from (a) to (c). The (0−6.5 MHz, 0−6.5 MHz) region is enlarged in the inset.

the flavin prosthetic group with the apoprotein (Eriksson et al., 1970; Kurreck et al., 1984). The respective structures of the neutral and anionic forms of the flavin semiquinone state are shown in Figure 5. The only structural difference between these two forms is the presence of a strongly coupled exchangeable proton at the N(5) position of the neutral flavin semiquinone. The strong coupling of this proton to the unpaired electron spin produces the neutral flavin semiquinone EPR spectrum to exhibit a peak-to-peak line width of ∼2 mT, while the anionic semiquinone shows a linewidth of ∼1.5 mT.

Due to the similarities found in the features seen in 1D-ESEEM and HYSCORE spectra of flavodoxin, FNR, and cholesterol oxidase in their semiquinone states (Figures 1−4), we can attribute them to interactions of the electronic spin with hydrogen and nitrogen nuclei present in the flavin ring semiquinone states. Another possibility would be an amino acid residue, either hydrogen-bonded or in close proximity to the flavin unpaired electronic spin. Nevertheless, it is unlikely that hydrogen and nitrogen nuclei in a protein environment would have transitions at frequencies as high as the ones shown here without contact interactions. Moreover, the crystallographic three-dimensional structures reported for this proteins show that, apart from the nitrogens of the flavin ring, there are no other reproducible structures in these proteins holding nitrogen atoms in the neighborhood of the flavin ring system. Isotopic labeling also confirmed the fact that all nitrogen and hydrogen nuclei that we have detect interacting with the unpaired spin belonged to the isoalloxazine flavin ring. The most naturally abundant isotopes of these nuclei, ^{1}H (natural abundance 99.985%) and ^{14}N (natural abundance 99.63%), have nuclear spins $I = {}^{1}/_{2}$ and $I = 1$, respectively. In [^{2}H]flavodoxin all exchangeable protons of the protein are replaced by ^{2}H which has $I = 1$. Among the protons replaced by ^{2}H, must be that bound to the nitrogen N(5) of the flavin ring in neutral semiquinones, as flavodoxin and FNR. In the [^{15}N]FMN flavodoxin sample all nitrogen nuclei in the flavin ring (positions 1, 3, 5, and 10 of the isoalloxazine ring) have been replaced by ^{15}N ($I = {}^{1}/_{2}$).

When all of these considerations are taken into account, the results shown above can be interpreted on the basis of the following spin Hamiltonian:

$$H = \beta g \vec{\mathbf{H}}\vec{\mathbf{S}} + \sum_i (H_n)_i \quad (1)$$

The first term accounts for the electronic Zeeman interaction, which in this case can be considered isotropic ($g \approx 2$, which implies a resonant magnetic field about 350 mT at X-band) with $S = {}^1/_2$. Calling S_ξ the component of the electronic spin in the quantification (static magnetic field) direction, it is also assumed that the energy splitting for the two electronic manifolds, $S_\xi = \pm{}^1/_2$, from that term is much larger than those due to the other relevant terms in the Hamiltonian (strong field approximation).

H_n gives the interaction terms of each nucleus:

$$H_n = H_z + H_{hf} + H_q = -\beta_N g_N \vec{\mathbf{H}}\vec{\mathbf{I}} + \vec{\mathbf{S}}\tilde{\mathbf{A}}\vec{\mathbf{I}} + \vec{\mathbf{I}}\tilde{\mathbf{P}}\vec{\mathbf{I}} \quad (2)$$

These three terms correspond respectively to nuclear Zeeman (z), hyperfine (hf), and quadrupolar (q) interactions. The quadrupolar term is only present when $I > {}^1/_2$. When the strong field hypothesis is taken into account, the hyperfine term can be taken as

$$H_{hf} = \langle S_\xi \rangle (l_x A_x I_x + l_y A_y I_y + l_z A_z I_z) \quad (3)$$

where $<S_\xi> = \pm{}^1/_2$ and l_x, l_y, and l_z are the director cosines of the external magnetic field vector with respect to the hf tensor principal axes. For the case of axial interaction, $A_x = A_y = A_\perp$, $A_z = A_\parallel$, and eq 3 can be rewritten as

$$H_{hf} = \langle S_\xi \rangle (AI_z + BI_x) \quad (4)$$

where

$$A = a + T(3\cos^2\theta - 1),\ B = 3T \sin\theta\cos\theta$$

$$a = \frac{2A_\perp + A_\parallel}{3},\ T = \frac{A_\parallel - A_\perp}{3} \quad (5)$$

$$A_\perp = a - T,\ A_\parallel = a + 2T$$

a and T being the isotropic and anisotropic hyperfine terms, and θ the angle between the (pseudo)dipolar hf tensor axis and the direction of the external magnetic field. The peaks observed in the frequency domain ESEEM spectra must correspond to transition frequencies of Hamiltonian (2). The HYSCORE correlation features in the frequency domain plane are displayed in position of frequencies corresponding to different electronic manifolds. On this basis, we shall study the main features found in spectra shown in Figures 2−4.

(a) Correlation Ridges at (7 MHz, 26 MHz)

The difference between the nuclear transition frequencies of the two manifolds in this ridge is compatible with a very high Larmor frequency. That points to a ^{1}H ($g_N = 5.586$, $\nu_L = 14.9$ MHz at 350 mT) as the nucleus responsible for this feature. The ridge can be seen in the neutral flavodoxin, the [^{15}N]FMN flavodoxin and the FNR semiquinone HYSCORE spectra, but is not present in those of neutral [^{2}H]flavodoxin and anionic cholesterol oxidase semiquinones. The absence of the ridge in the [^{2}H]flavodoxin confirms the fact that the signal is produced by a ^{1}H nucleus which is also exchangeable. This sample also shows low frequency features in the spectra that are attributed to a ^{2}H nucleus

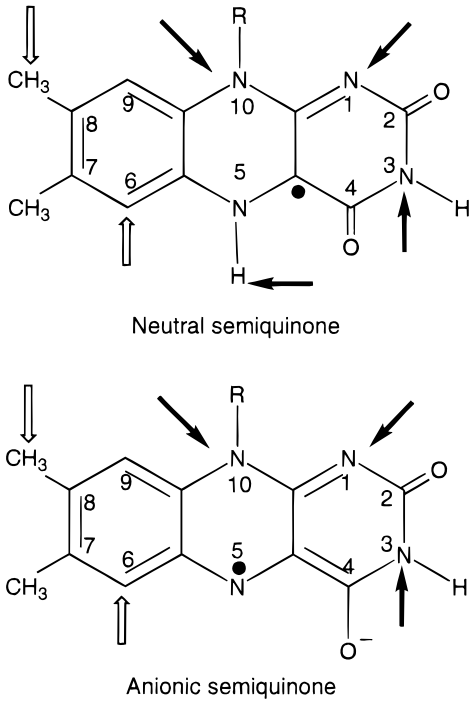

FIGURE 5: Structures of the neutral and anionic flavin semiquinone states. Arrows indicate positions of the isoalloxazine ring which interaction parameters with the unpaired spin have been unequivocally identified either by ENDOR (white arrows) or 2D-HYSCORE (black arrows) techniques in flavoprotein semiquinones.

strongly coupled to the spin. Moreover, the fact that this coupled ^{1}H nucleus is not seen in the HYSCORE spectrum of anionic cholesterol oxidase semiquinone suggests that the presence of such a ridge is directly related with a ^{1}H nucleus bound to the N(5) position in the neutral flavin semiquinone ring.

This correlation ridge was analyzed using the method described in the Appendix, showing that the hyperfine term can be considered axial. The parameters a and T (see eq 5) were estimated from the ridge positions, and more accurately determined using spectrum simulations. Two set of parameters are compatible with the observed HYSCORE signal, provided that exists an arbitrariness in the election of the manifold and angle that correspond to each transition (see Appendix). The corresponding values for these parameters obtained for flavodoxin and FNR semiquinone states are

Flavodoxin:

$a = -18.8 \pm 0.6$ MHz $\quad$ $a = 10.4 \pm 0.6$ MHz

or

$T = 8.7 \pm 0.3$ MHz $\quad$ $T = 8.7 \pm 0.3$ MHz

FNR:

$a = -18.7 \pm 0.8$ MHz $\quad$ $a = 10.4 \pm 0.8$ MHz

or

$T = 8.2 \pm 0.4$ MHz $\quad$ $T = 8.2 \pm 0.4$ MHz

The weak combination peak detected in the 33 MHz region of the flavodoxin and FNR semiquinone 4P spectra is also assigned to this interaction and is compatible with the values obtained for T (Dikanov & Tsvetkov, 1992b). Other signals from this nucleus would be too weak to be detected in a 1D-ESEEM experiment. Nevertheless, the ^{2}H nucleus bound to N(5) position in [^{2}H]flavodoxin semiquinone displays an

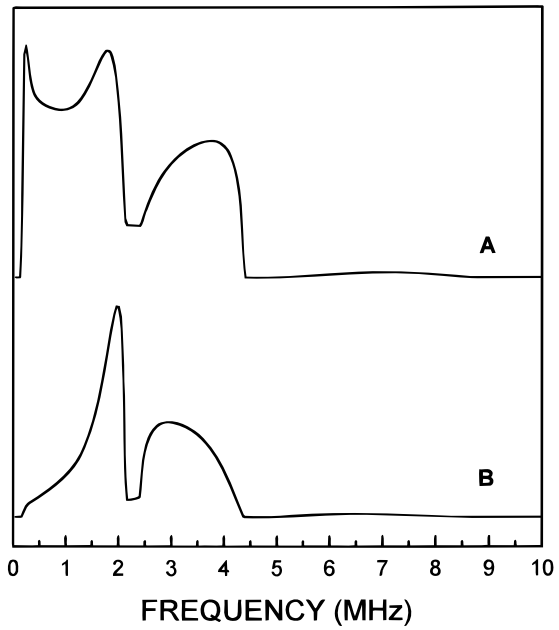

FIGURE 6: Computer simulation of the 3P 1D-ESEEM deuterium features in [^{2}H]flavodoxin for the two possible sets of parameters: (A) $a = -2.9$ MHz, $T = 1.3$ MHz; (B) $a = 1.6$ MHz, $T = 1.3$ MHz. Simulations include neither intrinsic width for signals nor quadrupolar term or spectrometer dead time effects. In spite of that, actual feature in the region between 0 and 2 MHz (see Figure 1) appears to be incompatible with simulation in B (see text).

intense 1D-ESEEM signal that can provide additional information in order to discriminate between the two parameter sets obtained for FNR and flavodoxin ^{1}H nucleus at the N(5) semiquinone position. The nuclear Zeeman and hyperfine interaction parameters of ^{2}H are proportional to those of ^{1}H following the Larmor frequencies ratio [$\nu_L(^2H) = 2.3$ MHz at 350 mT, $\nu_L(^2H)/\nu_L(^1H) = 0.153$]. Then, two sets of possible parameters for deuterium at N(5) position in flavodoxin semiquinone are also obtained:

$$a = -2.9 \pm 0.1 \text{ MHz} \qquad a = 1.6 \pm 0.1 \text{ MHz}$$
$$\text{or}$$
$$T = 1.3 \pm 0.1 \text{ MHz} \qquad T = 1.3 \pm 0.1 \text{ MHz}$$

The broad features between 0.5 MHz and 3 MHz in the 3P 1D-ESEEM and the combination peak at 5 MHz in the 4P 1D-ESEEM spectra of [^{2}H]flavodoxin correspond to the interaction with this nucleus (Figure 1). The position of signals is again compatible with both sets of parameters, but computer simulations of 3P spectra show different shapes in each case (Figure 6). The first set leads to a broad signal with noticeable intensity between 0.5 and 2 MHz, whereas for the second set this signal is rather an asymmetric peak, whose intensity strongly decreases below 1.5 MHz. Although the actual signal shape is affected by the deuterium quadrupolar term and the spectrometer dead time, the observed shape in the 3P spectrum of [^{2}H]flavodoxin is much better described by the first set ($a = -2.9$; $T = 1.3$). Moreover, this election is also supported by the parameters reported for hydrogen bound to N(5) in model flavins (Kurreck et al., 1984). A higher value for the hyperfine isotropic parameter of this interaction has also been suggested on the basis of CW-EPR experiments (Edmondson et al., 1990). Nevertheless, these authors considered in their analysis a nearly isotropic hyperfine term, which is not sustained by our results.

(b) Correlation Peaks at (3 MHz, 5 MHz)

This feature may be attributed to two nitrogen nuclei weakly interacting with the electronic spin. That excludes nitrogens at positions 5 and 10 of the flavin ring. It is known that there is a high electronic spin density on these positions, and their hyperfine interaction parameters, particularly the isotropic one, are quite large, about 20 MHz for N(5) and 10 MHz for N(10) (Kurreck, 1984; Edmondson, 1985). Therefore, the observed signals might be due to the other nitrogens in the isoalloxazine ring (positions 1 and 3), or to other nitrogen nuclei of the protein, out of the flavin ring but close to it. We have seen that labeling of flavodoxin FMN cofactor with ^{15}N isotope causes noticeable changes in the experimental features (Figure 2B). Correlation peaks (3 MHz, 5 MHz) can still be seen, but significantly reduced in intensity. Besides, other peaks at lower frequencies (1 MHz, 2 MHz) appear. Since only nitrogen nuclei in the flavin ring have been substituted by isotope labeling, the changes in spectra indicates that the observed signals must correspond to N(1) and N(3) of the isoalloxazine ring. The residual signal observed as correlation peaks (3 MHz, 5 MHz) can be interpreted as unlabeled ^{14}N(1) and ^{14}N(3), due to the fact that labeling with ^{15}N did not reach the 100% (see Materials and Methods). Some authors have suggested an isotropic hyperfine parameter for these nuclei about 1 MHz (Edmondson et al., 1990). In previous works, interaction parameters for N(1) and N(3) for cholesterol oxidase, flavodoxin, and FNR semiquinones were already described from 3P ESEEM experiments. Now, our HYSCORE measurements confirm the tentative assignment from 1D-ESEEM features to these nitrogens (Medina & Cammack, 1996; Medina et al., 1997).

These correlation peaks, (3 MHz, 5 MHz), observed in the HYSCORE experiments were also analyzed. Two narrow peaks, very close one to the other, can be observed. It is known that when ^{14}N ($I = 1$) interacts with an electronic spin in such a way that the isotropic hyperfine term dominates over the anisotropic and the quadrupolar terms, the frequency of the "double quantum" (dq) transitions ($\Delta I_z = \pm 2$) is nearly independent of the magnetic field orientation, and displays the most intense peaks in the ESEEM and HYSCORE spectra of orientationally disordered samples. If the isotropic hyperfine parameter matches the "exact cancellation" condition, $\nu_L = a/2$, three peaks, corresponding to the principal values of the quadrupolar tensor, are displayed coming from the cancelled electronic manifold. Besides, the dq peak of the other manifold must also be seen. Then, we propose that the observed correlation peaks correspond to dq−dq correlation of the two nitrogen nuclei at positions 1 and 3 of the isoalloxazine flavin ring. The absolute value of the isotropic hyperfine parameter, and some information about the quadrupolar tensor, can be obtained from the frequencies observed for these nuclei in the HYSCORE spectra (Dikanov & Tsvetkov, 1992c). Because we cannot assign a specific peak to a particular nucleus, N(1) or N(3), herein we will label the observed correlation peaks as N(A) and N(B). The hyperfine coupling constants (a), quadrupolar parameters (K), and asymmetry parameters (η) for cholesterol oxidase, FNR, and flavodoxin semiquinones are summarized in Table 1, where

$$K = \frac{|P_{z'}|}{2} = \left|\frac{e^2qQ}{4h}\right|, \eta = \left|\frac{P_{x'} - P_{y'}}{P_{z'}}\right| \qquad (6)$$

x', y', and z' being the principal directions of the quadrupolar tensor.

It is worthy to note that for some of the nitrogen nuclei observed in these flavoprotein semiquinones the isotropic hyperfine parameter cannot be considered dominant with respect to the quadrupolar term. However, simulations of 3P ESEEM spectra demonstrate that, as long as the anisotropic hyperfine term is small, the dq feature remains as a narrow, relatively intense peak (at least in one of the two electronic manifolds). In these cases the dq−dq correlation is still dominant in the HYSCORE spectrum.

For one of the nitrogen nuclei coupled to the spin in cholesterol oxidase semiquinone, the exact cancellation condition is nearly verified. In this case, the peak observed in the 3P ESEEM spectrum corresponds to the cancelled manifold and allows us to obtain the quadrupolar parameters for nucleus N(A) in cholesterol oxidase semiquinone. The obtained values for this nucleus are $K = 0.83 \pm 0.2$ MHz and $\eta = 0.5 \pm 0.1$. This value for the quadrupolar term (K) is slightly smaller than those reported (Lucken, 1969) for nitrogen in an isolated pyrimidine ring. Since peaks corresponding to N(A) in cholesterol oxidase semiquinone are quite narrow, it is likely that the anisotropic hyperfine term for N(A) in this sample is very small compared to the isotropic one. Just minor changes have been found for all the parameters calculated for cholesterol oxidase semiquinone HYSCORE spectra with regard to those already reported in 1D-ESEEM (Medina et al., 1997). Nevertheless, the improvement of the signal:noise ratio achieved by the 2D techniques, together with the higher resolution of the HYSCORE experiment as compared with 3P ones, give a better accuracy for the calculated parameter values. Having into account that the quadrupolar term is hardly influenced by changes in the ring far from the corresponding nucleus, values for quadrupolar parameters of N(A) in cholesterol oxidase semiquinone can be also considered a valid estimation for flavodoxin and FNR semiquinones.

To prove the correctness of our analysis, the frequencies for peaks corresponding to ^{15}N(A) and ^{15}N(B) in [^{15}N]FMN flavodoxin have been calculated. The rescaling of parameters for a ^{15}N ($I = {}^1/_2$) nucleus gives the following nuclear transitions:

$$\mathrm{N(A)}\begin{cases}\nu_\alpha = 2.5 \pm 0.3 \text{ MHz}\\ \nu_\beta = 0.5 \pm 0.2 \text{ MHz}\end{cases}$$

$$\mathrm{N(B)}\begin{cases}\nu_\alpha = 2.0 \pm 0.3 \text{ MHz}\\ \nu_\beta = 0.9 \pm 0.3 \text{ MHz}\end{cases}$$

The corresponding peaks can be observed in the [^{15}N]FMN flavodoxin semiquinone spectra. In 1D-ESEEM measurements two broad features in the regions of 1 MHz and 2 MHz are seen, whereas the HYSCORE spectrum shows a broad correlation at (1 MHz, 2 MHz)**.** Unfortunately, for the moment we are not in the position to assign each set of parameters to N(1) or N(3). Nevertheless, the possibility of assignation of these signals to other nuclei out of the flavin ring has been ruled out.

(c) Correlation Ridges in the Negative Quadrant

This feature of the HYSCORE spectra, that appears in all the flavoprotein semiquinones studied (Figures 2−4), shows a considerable change in shape when [^{14}N]FMN is replaced by [^{15}N]FMN in flavodoxin semiquinone (Figures 2A and 2B). This leads us to propose that it can be attributed to one of the flavin nitrogens. Since the analysis of $I = {}^1/_2$ signals has been shown to be easier, we will start analyzing the [^{15}N]FMN flavodoxin semiquinone HYSCORE spectrum following the method described in the Appendix. The ridge observed in this spectrum (Figure 2B) corresponds to an axial interaction with two compatible sets of parameters:

$$a = 15.9 \pm 1.4 \text{ MHz} \qquad a = -28.3 \pm 1.4 \text{ MHz}$$
$$\text{or}$$
$$T = 12.3 \pm 1.1 \text{ MHz} \qquad T = 12.3 \pm 1.1 \text{ MHz}$$

When these values are rescaled for the [^{14}N]FMN flavodoxin semiquinone the following data are obtained:

$$a = 11.7 \pm 1.0 \text{ MHz} \qquad a = -20.8 \pm 1.0 \text{ MHz}$$
$$\text{or}$$
$$T = 9.0 \pm 0.8 \text{ MHz} \qquad T = 9.0 \pm 0.8 \text{ MHz}$$

Isotropic hyperfine parameters have been determined for several flavin model compounds (Kurreck, 1984). The absolute value of a found in our first set of parameters is in the range of those reported for N(10) of the isoalloxazine ring, whereas the absolute value of a in the second set of parameters would be consistent with nitrogen N(5) of the same ring. Nevertheless, the sign of the isotropic parameter

Table 1: ^{1}H and ^{14}N Interaction Parameters of the Isoalloxazine Nuclei with the Unpaired Electronic Spin in the Semiquinone State of Different Flavoproteins

flavoprotein semiquinone	atom position	a (MHz)	T (MHz)	K (MHz)	η	$K^2(3+\eta)$ (MHz^2)
cholesterol oxidase	H(5)					
	N(A)[a]	1.9 ± 0.2[b]	nd	0.83 ± 0.2	0.5 ± 0.1	2.3 ± 0.2
	N(B)[a]	0.7 ± 0.2[b]	nd	nd	nd	2.1 ± 0.1
	N(10)	11.7 ± 1.0	9.0 ± 1.1	1.3[e]	nd	nd
FNR	H(5)	−18.7 ± 0.8	8.2 ± 0.4			
	N(A)[a]	1.2 ± 0.2[b]	nd	0.83 ± 0.2[c]	0.5 ± 0.1[c]	2.2 ± 0.1
	N(B)[a]	0.7 ± 0.3[b]	nd	nd	nd	2.4 ± 0.2
	N(10)	11.7 ± 1.0	9.0 ± 1.1	1.3[e]	nd	nd
flavodoxin	H(5)	−18.8 ± 0.6	8.7 ± 0.3			
	N(A)[a]	1.3 ± 0.3[b]	nd	0.83 ± 0.2[c]	0.5 ± 0.1[c]	2.2 ± 0.1
	N(B)[a]	0.8 ± 0.2[b]	nd	nd	nd	2.1 ± 0.1
	N(10)	11.7 ± 1.0	9.0 ± 1.1	1.3[d]	nd	nd

[a] These nitrogens correspond to N(1) or N(3) sites in the flavin ring. [b] Only the absolute value has been determined. [c] Estimated from values obtained for cholesterol oxidase. [d] Approximated value. [e] Estimated from value obtained for flavodoxin.

for N(5) has been reported for some flavin semiquinone model compounds as positive. Thus, this induces us to consider the first set of parameters as the correct solution, and to propose that our experimental features in the negative quadrant are due to the interaction of N(10) of the isoalloxazine ring with the unpaired electron. The hyperfine parameters obtained for N(10) in cholesterol oxidase, flavodoxin and FNR semiquinones are again summarized in Table 1.

For species with ^{14}N nuclei interacting with the electronic spin, dq−dq correlations corresponding to such a large a and T parameters must be too weak to be properly detected in the spectra. However, correlations between single quantum transitions (sq−sq) can be quite intense in some favourable orientations. N(10) sq−sq correlation ridges can be detected in the negative quadrant of the HYSCORE spectra of flavodoxin, FNR and cholesterol oxidase semiquinones. The different shape of these features with respect to that of [^{15}N]FMN flavodoxin is due to the quadrupolar interaction of $I = 1$ nuclei. Although the signal is detected for orientations with small effective hyperfine constant, in the highest frequency part the quadrupolar contribution can be considered weak compared to the other terms in the spin Hamiltonian, and a perturbative treatment following (Dikanov et al., 1995) can be applied. Our results are compatible with a quadrupolar parameter $K \approx 1.3$ MHz for flavodoxin semiquinone, being this value very close to those for nitrogen nuclei in isolated pyrazine rings (Lucken, 1969). If we suppose similar quadrupolar terms for the three flavoprotein semiquinones studied, the differences in frequency positions of the negative quadrant ridges can be associated to different hyperfine interactions. In any case, differences for hyperfine parameters Δa, $\Delta T < 0.3$ MHz are obtained, which are within our experimental error.

Figure 5 also shows a summary of the positions of the cholesterol oxidase, flavodoxin and FNR semiquinone states that have been unequivocally identified by the conjunction of ENDOR (Medina et al., 1994, 1995) and 2D-HYSCORE (present study) techniques. Six positions of the neutral isoalloxazine flavoprotein semiquinone ring are so far identified, N(1), N(3), H(5), H(6), CH_3(8), and N(10). All the same positions, except that of H(5) which does not exit in this case, have been identified in the anionic isoalloxazine ring of cholesterol oxidase semiquinone. The interaction parameters for these atoms with the electronic spin have also been calculated (Medina et al., 1994, 1995 and present study, Table 1). Since the identification of features in the spectra is already overcome, now the characterization of other flavoprotein semiquinones by these techniques must result much easier.

CONCLUSIONS

This study demonstrates that 1D- and 2D-ESEEM techniques, and in particular the HYSCORE spectroscopy, can be used for detecting and assigning nuclear transition frequencies in flavoprotein semiquinones. Isotopic ^{15}N labeling of FMN nitrogens in flavodoxin confirms that the ESEEM signals previously identified as arising from flavin nitrogen nuclei are due to the interaction of nitrogens N(1) and N(3) of the flavin isoalloxazine ring with the electronic spin of the semiquinone flavin state. The existence of a third stronger coupled nitrogen is also detected in HYSCORE spectra of flavoprotein semiquinones. Comparison of the coupling constants obtained for this nitrogen with those reported for model flavin compounds suggests that this signal is due to N(10) of the flavin ring. The presence of a strongly coupled proton has also been detected in the HYSCORE spectra of neutral flavoprotein semiquinones. This corresponds to the proton bound to N(5) position of the isoalloxazine ring, which is absent in anionic semiquinones. ENDOR studies provided information mainly on the electron density distribution of the benzene part of the flavin ring system. In the present study we have shown that for the study of flavoprotein semiquinones spin distribution 1D- and 2D-ESEEM spectroscopy is complementary to ENDOR studies, since it is offering information on the electron spin distribution on the pyrazine and pyrimidine rings of the isoalloxazine ring. Studies combining both techniques seem to be appropriated to detect changes on the electronic distribution of the flavin ring upon substrate binding. Moreover, they are also important tools for the study of mutated amino acid residues in the neighborhood of the isoalloxazine ring, which have been proposed to modulate the redox potential and the electronic properties of the flavin ring when bound to the apoprotein.

ACKNOWLEDGMENT

^{15}N-labeled FMN was a generous gift from Drs. J. Sancho and C. Genzor. We thank Professor David Blow from Imperial College, the Tokyo Research Laboratories of Kyowa Hakko Kogyo Ltd., Dr. Alice Vrielink from McGill University for providing a cholesterol oxidase sample, and E. J. Reijerse for simulation computer programs.

APPENDIX

Interaction with $I = {}^1/_2$ nuclei in the strong field approximation are described by the spin Hamiltonian given in eqs 1−3. The quadrupolar term does not appear. Frequencies for nuclear transitions are given by

$$\omega^2_{\alpha(\beta)} = \omega^2_{x\alpha(\beta)} l_x^2 + \omega^2_{y\alpha(\beta)} l_y^2 + \omega^2_{z\alpha(\beta)} l_z^2, \qquad \text{(A1)}$$

where

$$\omega_{i\alpha} = \left|\omega_N - \frac{A_i}{2}\right|, \; i = x, y, z$$
$$\omega_{i\beta} = \left|\omega_N + \frac{A_i}{2}\right|, \; i = x, y, z \qquad \text{(A2)}$$

$\omega_N = \beta_N g_N H$ is the Larmor frequency of the nucleus and

$$l_x = \sin\theta \cos\phi$$
$$l_y = \sin\theta \sin\phi \qquad \text{(A3)}$$
$$l_z = \cos\theta$$

are the director cosines of the external magnetic field direction with respect to the hf principal axes frame. θ is the colatitude angle, and ϕ is the azimuth one. In the case of axial hf interaction $A_x = A_y = A_\perp$, $A_z = A_{||}$, and expression (A1) becomes

$$\omega_\alpha^2 = \omega_{\perp\alpha}^2 + (\omega_{||\alpha}^2 - \omega_{\perp\alpha}^2)\cos^2\theta$$
$$\omega_\beta^2 = \omega_{\perp\beta}^2 + (\omega_{||\beta}^2 - \omega_{\perp\beta}^2)\cos^2\theta \quad \text{(A4)}$$

with

$$\omega_{i\alpha} = \left|\omega_N - \frac{A_i}{2}\right|, i = ||, \perp$$
$$\omega_{i\beta} = \left|\omega_N + \frac{A_i}{2}\right|, i = ||, \perp \quad \text{(A5)}$$

Parameters $A_{||}$ and $A_\perp$ are related with a and T by the expressions given in 5.

Following Dikanov and Bowman (1995), it is found that (ω_α^2, ω_β^2) plot of the $I = {}^1/_2$ HYSCORE signal in orientationally disordered systems provides a suitable test for determining whether the interaction is axial or rhombic, as well as a tool for estimating hyperfine interaction parameter values. The HYSCORE signal is obtained adding the contributions of all the possible orientations (all the possible values for θ and ϕ) which causes curved ridges and horn-shaped features in the conventional (ω_α, ω_β) plot. Such signals are difficult to analyze since the actually measured signal depends on the HYSCORE amplitude and usually only a restricted set of orientations are intense enough to be detected. Particularly, in the case of axial interaction, transitions for $\theta = 0$ and $\theta = \pi/2$ have zero intensity. Even when HYSCORE simulation computer programs are used in analysis, it is not easy to find good starting parameters. On the other hand, correlation features in a (ω_α^2, ω_β^2) plot are straight segments in the axial case, and triangles in the rhombic one (Dikanov & Bowman, 1995). Although the low amplitude of some orientations makes parts of the signal undetectable, those shapes in an (ω_α^2, ω_β^2) plot can be readily identified.

For axial interaction the straight line defined by the experimental segment allows us to obtain hf term parameters. From (A4)

$$\omega_\beta^2 = P + Q\omega_\alpha^2 \quad \text{(A6)}$$

where

$$P = \frac{\omega_{||\alpha}^2\,\omega_{\perp\beta}^2 - \omega_{\perp\alpha}^2\,\omega_{||\beta}^2}{\omega_{||\alpha}^2 - \omega_{\perp\alpha}^2}$$
$$Q = \frac{\omega_{||\beta}^2 - \omega_{\perp\beta}^2}{\omega_{||\alpha}^2 - \omega_{\perp\alpha}^2} \quad \text{(A7)}$$

This straight line can be characterized by the intersection points with the diagonal (ω_d^2, ω_d^2), horizontal ($\omega_{\alpha 0}^2$, 0), and vertical (0, $\omega_{\beta 0}^2$) axes, which are related with hf tensor parameters by

$$\omega_d^2 = \frac{P}{1-Q} = \omega_N^2 - {}^1/_4 A_{||}A_\perp$$
$$\omega_{\alpha o}^2 = -\frac{P}{Q} = 2(\omega_d^2)\Big/\left(1 + {}^1/_4\,\frac{A_{||} + A_\perp}{\omega_N}\right) \quad \text{(A8)}$$
$$\omega_{\beta o}^2 = P = 2(\omega_d^2)\Big/\left(1 - {}^1/_4\,\frac{A_{||} + A_\perp}{\omega_N}\right)$$

Using these relations, parameters $A_{||}$ and $A_\perp$ are obtained as the roots of the following equations:

$$X^2 \pm 4\omega_N\left|\frac{\omega_{\alpha o}^2 - \omega_{\beta o}^2}{\omega_{\alpha o}^2 + \omega_{\beta o}^2}\right|X + 4(\omega_N^2 - \omega_d^2) = 0 \quad \text{(A9)}$$

that can also be expressed as

$$X^2 \pm 4\omega_N\sqrt{1 - \left(\frac{2\omega_d^2}{\omega_{\alpha o}\omega_{\beta o}}\right)^2}\,X + 4(\omega_N^2 - \omega_d^2) = 0 \quad \text{(A10)}$$

The two signs of the linear term give valid solutions that correspond to a particular choice of the absolute sign in hf constants. Moreover, there exists another arbitrariness in assigning the roots of the equation (X_1, X_2) to $A_{||}$ or $A_\perp$. Then it leads to four possible sets of solutions. This corresponds with the experimental ambiguities of assigning the detected frequencies to transitions in manifold α or β and to orientation angle θ or $\pi/2-\theta$. The ambiguity is translated to the hf parameters in such a way that the four sets (a, T), ($-a - T$, T), ($-a$, $-T$) and ($a + T$, $-T$) are compatible with the fit of eq A4 to the observed HYSCORE signal. Only the absolute value of the anisotropy parameter is the same for all solutions. When a dipolar model for the hf interaction is assumed, T is defined as positive and then just two of the sets, (a, T) and ($-a - T$, T), remain as solutions. Spectral features for the two sets will have different HYSCORE intensities and in some favorable cases this will allow us to discriminate between both possibilities.

A similar method can be used for rhombic systems. Equations A.6 to A.9 can be applied for the three straight lines defined by the sides of the triangle feature in the (ω_α^2, ω_β^2) plot. In such a way the set (A_x, A_y, A_z) is obtained (except for a global change of signs).

REFERENCES

Bretz, N., Mastalsky, I., Elsner, M., & Kurreck, H. (1987) *Angew. Chem., Int. Ed. Engl. 26*, 345−347.

Bruns, C. M., & Karplus P. A. (1995) *J. Mol. Biol. 247*, 125−145.

Cavener, D. R. (1992) *J. Mol. Biol. 223*, 811−814.

Correll, C. C., Ludwig, M. L., Bruns, C. M., & Karplus, P. A. (1993) *Protein Sci. 2*, 2112−2133.

Dikanov, S. A., & Tsvetkov, Yu. D. (1992a) in *Electron Spin Echo Envelope Modulation (ESEEM) Spectroscopy*, pp 225−226, CRC Press, Boca Raton, FL.

Dikanov, S. A., & Tsvetkov, Yu. D. (1992b) in *Electron Spin Echo Envelope Modulation (ESEEM) Spectroscopy*, p 115, CRC Press, Boca Raton, FL.

Dikanov, S. A., & Tsvetkov, Yu. (1992c) in *Electron Spin Echo Envelope Modulation (ESEEM) Spectroscopy*, pp 187ff, CRC Press, Boca Raton, FL.

Dikanov, S. A., & Bowman, M. K. (1995) *J. Mag. Reson., Ser. A 116*, 125−128.

Dikanov, S. A., Tyryshkin, A. M., Hüttermann, J., Bogumil, R., & Witzel, H. (1995) *J. Am. Chem. Soc. 117*, 4976−4986.

Dikanov, S. A., Xun, L., Karpiel, A. B., Tyryshkin, A. M., & Bowman, M. K. (1996) *J. Am. Chem. Soc. 118*, 8408−8416.

Edmondson, D. E. (1985) *Biochem. Soc. Trans. 13*, 593−600.

Edmondson, D. E., & Tollin, G. (1983) *Top. Curr. Chem. 108*, 107−138.

Edmondson, D. E., & McCormick, D. B., Eds. (1987) *Flavins and Flavoproteins*, Walter de Gruyter, Berlin.

Edmondson, D. E., Müller, F., Schaub, F., & Nisimoto, Y. (1990) in *Flavins and Flavoproteins* (Curti, B., Ronchi, S., & Zanetti, G., Eds.) pp 67−72. Walter de Gruyter, Berlin.
Eriksson, L. E. G., Ehrenberg, A., & Hyde, J. S. (1970) *Eur. J. Biochem. 17*, 539−543.
Fillat, M. F., Sandmann, G., & Gómez-Moreno, C. (1988) *Arch. Mircrobiol. 150*, 160−164.
Fillat, M. F., Edmondson, D. E., & Gómez-Moreno, C. (1990) *Biochim. Biophys. Acta 1040*, 301−307.
Fillat, M. F., Borrias, W. E., & Weisbeerk, P. J. (1991) *Biochem. J. 280*, 187−191.
Genzor, C. G., Belbarrain, A., Gómez-Moreno, C., López-Lacomba, J. L., Cortijo, M., & Sancho, J. (1996) *Protein Sci. 5*, 1376−1388.
Gómez-Moreno, C., Martínez-Júlvez, M., Fillat, M. F., Hurley, J., & Tollin, G. (1995) in *Photosynthesis: From Light to Biosphere* (Mathis, P., Ed.) Vol. 2, pp 627−632, Kluwer Academic Publishers, The Netherlands.
Höfer, P., Grupp, A., Nebenführ, H., & Mehring, M. (1986) *Chem. Phys. Lett. 132*, 279−282.
Inouye, Y., Taguchi, K., Fuji, A., Ishimaru, K., Nakamura, S., & Nomi, R. (1982) *Chem. Pharm. Bull. 30*, 951−958.
Janot, J.-M., Capeillere-Blandin, C., & Labeyrie, F. (1990) *Biochem. Biophys. Acta 1016*, 165−176.
Kamei, T., Takiguchi, Y. Suzuki, H., Matsuzaki, M., & Nakamura, S. (1978) *Chem. Pharm. Bull. 26*, 2799−2804.
Karplus, P. A, Daniels, M. J., & Herriott, J. R. (1991) *Science* 251, 60−66.
Knaff, D. B., & Hirasawa, M. (1991) *Biochim. Biophys. Acta 1056*, 93−125.
Kofman, V., Shane, J. J., Dikanov, S. A., Bowman, M. K., Libman, J., Shanzer, A., & Goldfarb, D. (1995) *J. Am. Chem. Soc. 117*, 12771−12778.
Kofman, V., Farver, O., Pecht, I., & Goldfarb, D. (1996) *J. Am. Chem. Soc. 118*, 1201−1206.
Kurreck, H., Bock, M., Bretz, N., Elsner, M., Kraus, G., Lubitz, W., Müller, F., Geissler, H., & Kroneck, P. M. H. (1984) *J. Am. Chem. Soc. 106*, 737−746.
Kurreck, H., Kirsrte, B., & Lubitz, W. (1987) in *Electron Nuclear Double Resonance Spectroscopy of Radicals in Solution.* (Marchand, A. P., Ed.) pp 308−327. VCH, Weinheim.
Li, J., Vrielink, A., Brick, P., & Blow, D. M. (1993) *Biochemistry 32*, 11507−11515.
Lucken, E. A. C. (1969) in *Nuclear Quadrupole Coupling Constants*, p 217ff, Academic Press, London.
Medina, M., & Cammack, R. (1996) *J. Chem. Soc., Perkin Trans. 2*, 633−638.
Medina, M., Vrielink, A., & Cammack, R. (1994) *Eur. J. Biochem. 222*, 941−947.
Medina, M., Gómez-Moreno, C., & Cammack, R. (1995) *Eur. J. Biochem. 227*, 529−536.
Medina, M., Vrielink, A., & Cammack, R. (1997) *FEBS Lett. 400*, 247−251.
Mims, W. V., & Peisach, J. (1981) in *Biological Magnetic Resonance* (Berliner, L. J., & Reuben, J., Eds.) pp 213−263, Plenum, New York.
Müller, F. (1983) *Top. Curr. Chem. 108*, 71−107.
Pueyo, J. J., & Gómez-Moreno, C. (1991) *Prep. Biochem. 21*, 191−204.
Pueyo, J. J., Gómez-Moreno, C., & Mayhew, S. G. (1991) *Eur. J. Biochem. 202*, 1065−1071.
Rogers, L. J. (1987) in *The Cyanobacteria* (Fay, P., & Van Baslen, C., Eds.) Elsevier Science Publishers, Amsterdam.
Schweiger, A. (1990) in *Modern Pulsed and Continuous-Wave Electron Spin Resonance* (Kevan, L., & Bowman, M. K., Eds.), p 43ff, J. Wiley and Sons, New York.
Serre, L., Vellieux, F. M. D., Medina, M., Gómez-Moreno, C., Fontecilla-Camps, J.C., & Frey, M. (1996) *J. Mol. Biol. 263*, 20−39.
Shane, J. J., van der Heijden, P. A. A. W., Reijerse, E. J., & de Boer, E. (1994) *Appl. Magn. Res. 6*, 427−454.
Shergill, J. K., Joannou, C. L., Mason, J. R., & Cammack, R. (1995) *Biochemistry 34*, 16532−16542.
Smith, A. G., & Brooks, C. J. W. (1975) *Biochem. Soc. Trans. 3*, 675−677.
Tsvetkov, Y. D., & Dikanov, S. A., (1987) in *Metal Ions Biol. Syst. 22*, 207−263.
Uwajima, T., Yagi, H., Nakamura, S., & Terada, O. (1973) *Agric. Biol. Chem. 37*, 2345−2350.
Uwajima, T., Yagi, H., & Terada, O. (1974) *Agric. Biol. Chem. 38*, 1149−1156
Vrielink, A., Lloyd, L. F., & Blow, D. M. (1991) *J. Mol. Biol. 219*, 533−554.
White, P., Manson, F. D. C., Brunt, C. E., Chapman, S. K., & Reid, G. A. (1993) *Biochem. J.* 291, 89−94.
Yagi, K., Ed. (1993) *Flavins and Flavoproteins*, Walter de Gruyter, Berlin.

BI971495G